excited states (**2****) proceeds by a sequential bond-scission mechanism. Low temperature to reduce the internal conversion rate and intense irradiation for two-photon processes to occur appear to be necessary for the isomerization to proceed efficiently. On the basis of the spectra and kinetics it appears that the reverse reaction (**1**** → **2***) is unimportant.

Very weak or no long-lived emission associated with **3S*** was observed in xenon matrices, indicating that the **3S*** lifetime must be ≲10 ns. This strongly supports the hypothesis (ref 9) that in the absence of chemical reactions intersystem crossing to a triplet state is the main **3S*** depletion mechanism and is facilitated by the external heavy atom effect induced by the xenon matrix. Other possible depletion channels within the singlet mainfold, such as additional isomerization or ring closure to **4**, would be expected to be relatively insensitive to the nature of the matrix.

Summary and Conclusions

High-intensity picosecond UV photolysis of diazenes **1** or **2** lead to the excited singlet TMM ($^1A_1$) **3S***. The inert matrix isolation data indicates the parent diazene absorbs two photons and is excited to the S_n state, from which dissociation to **3S*** occurs. At 4.2 K the highly excited **2**** can also rearrange to give **1*** as indicated by both kinetics and spectra.

This rearrangement suggests that low-temperature laser-induced photodeazetation of **2** proceeds through a sequential C-N bond scission mechanism. In room-temperature hexane solution no isomerization of **1** or **2** is observed, indicating that under these conditions internal conversion to the lowest excited singlet state is much faster than isomerization.

The TMM formed (**3S***) has its main emission spectrum band at 445 nm. Its fluorescence lifetime was found to vary from ~300 ps at room temperature to ~30 ns in 4.2 K argon matrices.

This low-temperature lifetime was reduced to <10 ns in 4.2 K xenon matrices. This is interpreted as indicating that in the absence of chemical reactions intersystem crossing to the triplet manifold is the dominant quenching mechanism of the excited singlet TMM.

Acknowledgment. The authors thank E. F. Hilinski for many helpful discussions, and Professor Jerome Berson and M. R. Mazur for providing the diazene samples.

Registry No. 1, 31689-32-4; **2**, 38136-44-6; **3**, 32553-01-8; argon, 7440-37-1; xenon, 7440-63-3.

Photoelectron–Photoion Coincidence Spectroscopy as a Sensitive Probe for RRKM Calculations: Are the Lowest Energy Fragmentation Pathways of 1,3-Butadiene Cation in Effective Competition?

Rolf Bombach, Josef Dannacher,* and Jean-Pierre Stadelmann

Contribution from the Physikalisch-Chemisches Institut der Universität Basel, CH-4056 Basel, Switzerland. *Received September 13, 1982*

Abstract: The low-energy breakdown diagram of 1,3-butadiene cation has been measured and calculated, by using He Iα photoelectron–photoion coincidence spectroscopy and RRKM theory, respectively. Formation of $C_2H_4^+$ cannot be in effective competition with the other three energetically accessible reactions leading to $C_3H_3^+$, $C_4H_5^+$, and $C_4H_4^+$ fragment ions. At least in the threshold region of the lowest energy fragment, 1,3-butadiene cation in its electronic ground state must be the reactant, since none of the higher energetic isomers can provide the high density of states required to explain the experimentally observed low decay rates. The rate–energy functions for the three competing dissociations are established. This allows the determination of the respective threshold energies, even for $C_4H_4^+$ formation where a considerable competitive shift is operating. The transition states involved are found to be tighter than the reactant, in accord with the known structures of the products demanding a cyclization in the course of all three processes. Preexponential factors and activation entropies are inferred for a possible comparison with the results of classical kinetics.

Many practical, interesting chemical reactions are complex in the sense that they involve a few discrete steps termed elementary reactions, which for the most part correspond to unimolecular or bimolecular processes. Unimolecular reactions involving merely a single, isolated, suitably activated species reacting by isomerization or decomposition are the simplest elementary processes conceivable and, therefore, of fundamental importance in chemistry.[1]

The earliest efforts to calculate the unimolecular rate constant from the intrinsic properties of the excited reactant were instigated by a wealth of experimental data on gas-phase reactions assumed to be unimolecular processes.

Owing to Lindemann's[2] famous theory, it soon became apparent that there was no one-to-one correspondence between the experimentally determined reaction order and the molecularity of a process. It was also recognized that the experimental first-order rate "constant" for unimolecular reactions involving collisional energization and deactivation was only a pseudoconstant, declining at sufficiently low pressures. This "fall-off" or Lindemann effect of the experimental rate constant has since become a valuable criterion for the presence of a truly unimolecular reaction, brought about by collisional activation. Though it was confirmed that at high pressures the experimental first-order rate constant was a quantity independent of concentration, Lindemann's work evidenced that this constant was not identical with the unimolecular rate constant. In the field of classical gas-phase kinetics, two major

(1) Forst, W. "Theory of Unimolecular Reactions"; Academic Press: New York, 1973. Robinson, P. J.; Holbrook, K. A. "Unimolecular Reactions"; Wiley-Interscience: New York, 1972.

(2) Lindemann, F. A. *Trans. Faraday Soc.* **1922**, *17*, 598.

0002-7863/83/1505-1824$01.50/0

factors prevent the desired direct measurement of the unimolecular rate constant. Firstly, collisional activation leads to a broad energy distribution of the reacting molecules, blurring the energy dependence of the quantities involved. Secondly, the unimolecular reaction of interest takes place in competition with collisional deactivation.

In this respect, more recently developed experimental techniques for ionic systems[3] provide a direct and much more sensitive way to test the statistical theories of unimolecular reactions.[4] Compared with classical kinetics these experiments are favored by the greater ease with which ions can be manipulated and detected as well as the absence of collisional phenomena. The conclusions derived from studies on charged species should be transferable to comparable neutral systems.

One of the most valuable techniques for probing the unimolecular decay of internal-energy-selected molecular cations is photoelectron–photoion coincidence spectroscopy. Several versions[5-7] of this young experimental method have been used to measure unimolecular rate constants as a function of the internal energy of the initially generated parent ions. Most studies were concerned exclusively with the lowest energy fragmentation pathway. Lately, the dissociation of iodobenzene cation into phenyl cation plus iodine radical has been extensively investigated by employing three different coincidence spectrometers with sampling times covering almost 2 orders of magnitude.[8] Taking carefully into account the thermal energy content of the photoionized molecules and the apparatus functions of the instruments used, the rate–energy dependence of this dissociation reaction was precisely determined. The rate constant of the process in question was also calculated applying RRKM theory.[4] The different models used were kept as simple as possible, involving only two adjustable parameters. These two parameters—the critical energy of the process and a quantity related to the level density of the transition state—could be derived by a nonlinear regression technique from the extended set of experimental data. Excellent agreement between calculated and measured data was obtained for reasonable values of the parameters.

The described analysis of photoelectron–photoion coincidence data by means of RRKM theory is not confined to the lowest energetic fragmentation channel of an excited molecular cation. The present study is concerned with an extension of this method to several competing dissociations using the four least endothermic fragmentation reactions of 1,3-butadiene cation as an illustrative example. Several years ago, the rate–energy function of the lowest energy fragmentation pathway of this species was investigated in one of the pioneering photoelectron–photoion coincidence studies.[5] In that article it was found that the statistical theory failed to account for the measured values, which had been inferred from the asymmetrically broadened time-of-flight distributions of the $C_3H_3^+$ fragment ions. However, this method of coincidence data analysis has since become questionable as the deduced rates disagreed significantly in several independent cases[8,9] with the outcome of an alternative and more straightforward data evaluation technique relying on time-resolved measurements of branching ratios. Recently, the origin of this discrepancy could be attributed to an erroneous effective sampling function used to analyse the earlier data.[10] Therefore, the present study represents also an attempt to reexamine the low-energy-decay behavior of an important organic cation by proved experimental and theoretical means.

Experimental Section

The He Iα photoelectron–photoion coincidence spectrometer used in this study has previously been described in greater detail.[11] Therefore, only those experimental aspects are recalled that are most pertinent to the present work.

The sampling function of the electron energy analyzer can be characterized by a Gaussian with a full width at half maximum of 120 meV. The electron transmission coefficient amounts to $f_e \approx 10^{-4}$. As a quadrupole mass filter is used in the ion channel, the required mass resolving power is ensured and relatively high ion transmission coefficients ($f_i \approx 0.2$–0.3) can nevertheless be achieved. The lapse of time between formation and detection of the generated photoions can be varied. This makes it possible to study the dependence of the breakdown diagram on the experimental time scale and, thus, the lifetime of the initially generated molecular cations.

Results and Discussion

A. Essence of Branching Ratios. The concept of branching ratios will be recapitulated inasmuch as the following analysis is based on these quantities.[12] By definition, and referring to a particular ionization energy I, the branching ratio $b[I,m_k]_t$ denotes the number of molecular or fragment ions with "mass" m_k detected after the experimental sampling time t, relative to the total number of initially ($t = 0$) produced molecular ions. These branching ratios can be obtained unambiguously from electron–ion coincidence measurements only in those cases where the corresponding ion transmission coefficients $f_i(m_k)$ are precisely known, since solely the product of $f_i(m_k)$ with $b[I,m_k]_t$ can be derived directly from the respective coincidence signal. The ion transmission coefficient in its turn depends on the mass to charge ratio and the kinetic energy distribution of the ions in question. Moreover, the ion transmission coefficient of fragment ions may even become a function of the fragmentation rate constant if the dissociative lifetime is comparable to the sampling time of the experiment.[13] The ion transmission coefficient for molecular ions can be determined unequivocally because their translational energy distribution is always thermal, independent of their internal energy content. Therefore, it suffices to measure $f_i(m_k) \times b[I,m_k]_t$ at a single ionization energy I where dissociations cannot take place for energetic reasons and, accordingly, $b[I,m_k]_t$ must be equal to unity. As soon as the value of $f_i(m_k)$ has been ascertained, the parent-ion branching ratio can be obtained precisely at any ionization energy I within the energy range provided by the light source used. The situation is much more involved when fragment ions are considered, since their kinetic energy distribution depends generally on the available excess energy of the precursor and, thus, on the ionization energy I. The larger the amount of the kinetic energy carried away by the charged fragment the lower the value of $f_i(m_k)$, relative to the ion transmission coefficient for a thermal ion of the same mass to charge ratio. Currently, only semiquantitative methods are available for determining the fragment ion transmission coefficients in the most general case. As a consequence, the attainable precision for the corresponding branching ratios is mostly lower for fragment ions than for molecular ions and the experimental data are not self-normalizing in the strict sense.

Two different methods of coincidence data analysis are presently in use in order to provide the breakdown diagram in a normalized form, which is prerequisite to any theoretical treatment. A first method completely ignores the dependence of $f_i(m_k)$ on the mass to charge ratio and on the kinetic energy distribution of the ions considered. The branching ratios are directly equated to the relative areas of the respective coincidence signals. This method, usually applied in threshold photoelectron–photoion coincidence spectroscopy,[14] tends to underestimate the branching ratio of fragment ions that carry a great deal of kinetic energy. Considering ions of a given "mass" m_k, the second more elaborate method initially approximates $f_i(m_k)$ by the known value for ions

(3) "Gas Phase Ion Chemistry"; Bowers, M. T., Ed.; Academic Press: New York, 1979.
(4) Marcus, R. A.; Rice, O. K. *J. Phys. Colloid Chem.* **1951**, *55*, 894.
(5) Werner, A. S.; Baer, T. *J. Chem. Phys.* **1975**, *62*, 2900.
(6) Stockbauer, R.; Rosenstock, H. M. *Int. J. Mass Spectrom. Ion Phys.* **1978**, *27*, 185.
(7) Dannacher, J.; Schmelzer, A.; Stadelmann, J.-P.; Vogt, J. *Int. J. Mass Spectrom. Ion Phys.* **1979**, *31*, 175.
(8) Dannacher, J.; Rosenstock, H. M.; Buff, R.; Parr, A. C.; Stockbauer, R. L.; Bombach, R.; Stadelmann, J.-P. *Chem. Phys.* **1983**, in press.
(9) Baer, T.; Tsai, B. P.; Smith, D.; Murray, P. T. *J. Chem. Phys.* **1976**, *64*, 2460. Rosenstock, H. M.; Stockbauer, R.; Parr, A. C. *Ibid.* **1979**, *71*, 3708; **1980**, *73*, 773.
(10) Baer, T., private communication.
(11) Dannacher, J.; Vogt, J. *Helv. Chim. Acta* **1978**, *61*, 361.
(12) Stadelmann, J.-P. Ph.D. Thesis, University of Basel, 1981.
(13) Stadelmann, J.-P.; Vogt, J. *Int. J. Mass Spectrom. Ion Phys.* **1980**, *35*, 83.
(14) Parr, A. C.; Jason, A. J.; Stockbauer, R. *Int. J. Mass Spectrom. Ion Phys.* **1978**, *26*, 23.

Table I. Relevant Thermochemical Data[a]

	neutral			cation		
	$\Delta_f H^\ominus_0$(g) kJ mol^{-1}	$\Delta_f H^\ominus_{298}$(g), kJ mol^{-1}	ionization energy, eV	$\Delta_f H^\ominus_0$(g), kJ mol^{-1}	$\Delta_f H^\ominus_{298}$(g), kJ mol^{-1}	calculated 0 K thresholds,[b] eV
C_4H_6[c]	123.6[d]	108.8[e]	9.060	997.8	983.0	
C_4H_5				1013.0[f]	1003.0	11.46
C_4H_4				1195.0[g]	1185.0[h]	11.10
C_3H_3				1085.0[f]	1075.0	11.47
C_2H_4	60.7	52.3	10.500	1073.8	1065.4	12.20
C_2H_2	227.3	226.7				
CH_3	145.6	142.3				
H	216.0	218.0				

[a] Data drawn from ref 23 in the absence of other citations. [b] For the formation from 1,3-butadiene, assuming the reactions given in the text. [c] 1,3-Butadiene. [d] Conversion of the corresponding room-temperature value to 0 K using the vibrational frequencies given in ref 17 and approximate enthalpy function of ref 24. [e] Reference 25. [f] Estimated from corresponding room-temperature value. [g] Reference 26. [h] Estimated from corresponding 0 K value.

with a thermal kinetic energy distribution. This yields lower limits for the branching ratios of the fragment ions, because the actual value of $f_i(m_k)$ cannot be larger than its thermal counterpart. When these approximate branching ratios are added up for each ionization energy I, the so-called sum curve is obtained. The deviation of this sum curve from its theoretical value unity evidences directly the extent of the reduction of the ion transmission coefficients due to high-kinetic-energy fragment ions. This overall loss of collection efficiency can then be partitioned among the individual fragmentation channels involved, provided that the average translational energy of the fragments formed is also measured as a function of I and the apparatus function of the spectrometer is sufficiently well-known. When erroneous ion transmission coefficients as a significant error source are eliminated, a corrected breakdown diagram can be derived. This second more accurate but also more cumbersome way of data evaluation is the method of choice, in particular when fixed wavelength coincidence data are analysed.[12] The breakdown diagram presented in Figure 1 has been obtained by applying this second way of coincidence data analysis.

Aiming at a quantitative description of the breakdown diagram of 1,3-butadiene cation by means of RRKM calculations, we had to confine the ionization energies in the present work to within the range of I = 9 to 13 eV since there is evidence for nonstatistical behavior at higher values of I.[15] Accordingly, the molecular ions are initially formed in one of the lowest three electronic states, i.e., $\tilde{X}\ ^2B_g$, $\tilde{A}\ ^2A_u$, $\tilde{B}\ ^2A_g$, corresponding to the first three bands (the circled numbers) of the photoelectron spectrum, as depicted in Figure 1. He Iα photoionization to the electronic ground state and to the lowest vibrational levels of the electronic $\tilde{A}$ state leads exclusively to stable 1,3-butadiene cations, whereas excitation to higher vibrational levels of the electronic $\tilde{A}$ state or to the electronic $\tilde{B}$ state is followed by dissociative processes (cf. Figure 1). The following four fragmentation channels are accessible within the energy range considered:

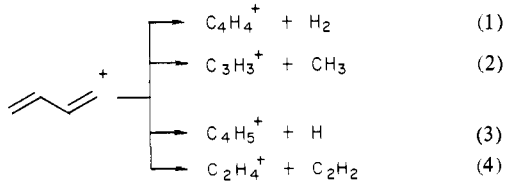

Reliable upper bounds for the thermochemical thresholds for $C_4H_4^+$ and $C_3H_3^+$ production are known, and the dissociation limit for the formation of $C_2H_4^+$ is exactly established. The calculated threshold energy for the $C_4H_5^+$ fragment ion according to reaction 3 involves a little bit more ambiguity. The relevant thermochemistry is summarized in Table I.

B. Basic Assumptions of RRKM Theory. Quite generally, statistical theories of unimolecular reactions can only be expected to account properly for the decay of excited molecular cations if several inescapable conditions are satisfied.[1] First of all, it is presupposed that any electronic excitation energy of the initially generated molecular ions is converted into vibrational energy of the electronic ground state by radiationless transitions, which are much faster than the actual dissociative steps. There are ex-

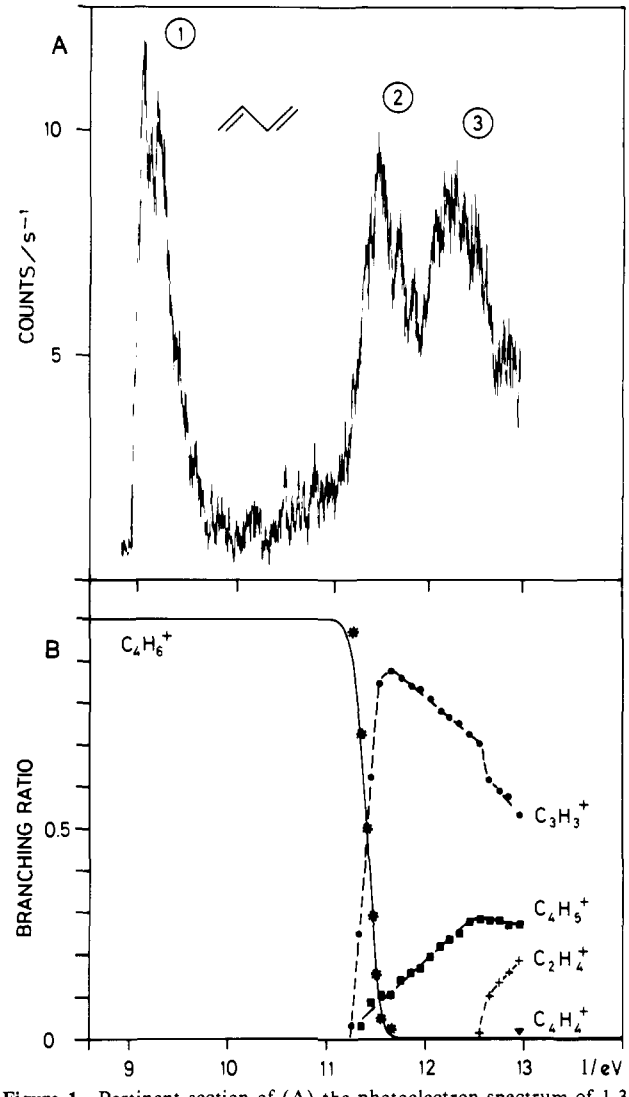

Figure 1. Pertinent section of (A) the photoelectron spectrum of 1,3-butadiene recorded under coincidence conditions and (B) the experimental breakdown diagram: (*) $C_4H_6^+$, (●) $C_3H_3^+$, (■) $C_4H_5^+$, (+) $C_2H_4^+$, (▼) $C_4H_4^+$. The solid line represents the calculated breakdown curve for the molecular ion, based on the best fit of the linear transition state model with σ = 1 and τ_{exp} = 28 μs, i.e., corresponding to curve b in Figure 2.

(15) Dannacher, J.; Flamme, J.-P.; Stadelmann, J.-P.; Vogt, J. *Chem. Phys.* **1980**, *51*, 189.

perimental observations that imply that this holds true for the first excited electronic state of 1,3-butadiene cations. To begin with, the dipole-allowed radiative transition $\tilde{A}\ ^2A_u \rightarrow \tilde{X}\ ^2B_g$ is absent ($\Phi \leq 10^{-5}$),[16] indicating a rapid ($k_{IC} > 10^{11}\ s^{-1}$) depopulation of the electronic $\tilde{A}$ state by nonradiative processes. Furthermore, the lack of resolvable fine structure of the corresponding photoelectron band is also consistent with a fast depletion of the $\tilde{A}\ ^2A_u$ state by internal conversion.

The applicability of statistical theories of unimolecular reactions further necessitates that the vibrational energy is randomized among the internal degrees of freedom and that the available energy is the necessary and sufficient criterion for reaction. The energetically accessible fragmentation reactions, which are presumed to compete effectively on the ground-state manifold, can then be described by time-independent rate constants equivalent to the one-dimensional passage of a system point over an energy barrier. The total decay rate of the precursor is given by the sum of the individual rate constants.

As outlined in the following sections, these assumptions are compatible with our results on reactions 1–3 but are in contradiction to our coincidence data for reaction 4. It is also recalled that in order to calculate unimolecular rate constants by means of statistical theories, rather concrete assumptions have to be made about the structure and the intrinsic properties of both, the reactant and the transition state. In the present case, the measured rates indicate that at least in the threshold region of the first three processes, 1,3-butadiene cation in its electronic ground state is the precursor ion. For principal reasons, the assumptions concerning the transition state and the choice of the reaction coordinate usually rely almost completely on chemical intuition. Therefore, in order for one to put the formulation of transition-state structures, nevertheless, on a rational basis, the models used should be kept as simple as possible,[1] e.g., as outlined in most recent work on iodobenzene cation.[8]

C. Outline of the Computations. According to RRKM theory, the individual rate–energy dependencies of competitive unimolecular fragmentations can be described by expressions of the form:

$$k^i(E^* - E_0^i) = \sigma^i \frac{W^{\ddagger i}(E^* - E_0^i)}{h\rho(E^*)}$$

provided that all the mentioned underlying assumptions are correct. The index i refers to one of the four processes given above, whereas σ^i represents the reaction path degeneracy.[1] E^*, E_0^i, $\rho(E^*)$, and $W^{\ddagger i}(E^* - E_0^i)$ denote respectively the available excess energy, the critical energy of reaction i, the density of states of the precursor with internal energy E^*, and the integrated density of states of the transition state for process i taken between threshold and $E^* - E_0^i$. Already, a preliminary analysis showed that in order to account for the coincidence results, threshold rates on the order of $10^3\ s^{-1}$ are required for the lowest energy process. Consequently, E^* must be large enough so that $\rho(E^*)$ in turn can reach values on the order of 10^9 states per wavenumber.[1] Therefore, the precursor is identified with 1,3-butadiene cation in its $\tilde{X}\ ^2B_g$ state, since only this $C_4H_6^+$ species can provide such a high-level density at the energies in question. This assignment is also retained at higher excitation energies, as long as the respective results remain compatible with the experimental data. The vibrational frequencies were approximated by the corresponding values of the parent neutral.

Linear and cyclic transition-state structures have been probed, by using the frequencies of 1,3-butadiene[17] and methylcyclopropene[18] multiplied by an adjustable, constant factor F^i. The reaction coordinates were a C–C stretching mode for the processes 2 and 4 and a C–H stretching vibration in the case of the other two reactions. Moreover, the effect of a reaction path degeneracy of two has also been studied. Following the coarse graining of all the energy quantities involved in 5-meV intervals, level densities and their sums were evaluated by means of exact count algorithms. Rate–energy functions were computed for given initial values of E_0^i and F^i. The corresponding breakdown curves were then derived by carefully accounting for the time scale and the effective sampling function of the experiment.[8] The experimental data were fit with these calculated breakdown curves. The most recently applied regression technique was extended to the case of several competing reactions, using E_0^i and F^i as adjustable parameters.

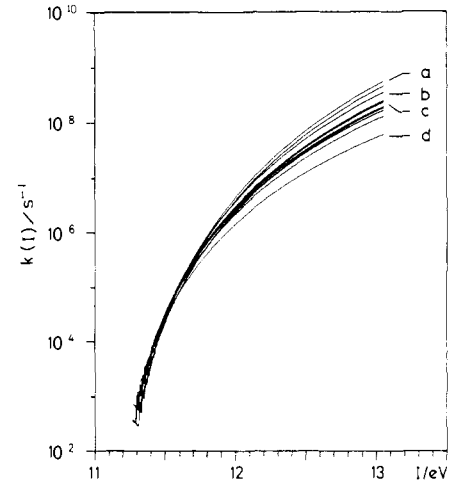

Figure 2. Approximate total rate–energy functions derived exclusively from the parent ion data: (a) $\sigma = 1$, $\tau_{exp} = 70\ \mu s$; (b and c) $\sigma = 1$, $\tau_{exp} = 28\ \mu s$; (d) $\sigma = 2$, $\tau_{exp} = 45\ \mu s$. Curves a, b, and d refer to a linear and curve c to a cyclic transition-state model.

D. Results Derived from the Molecular Ion Data. The parent-ion breakdown curve has been measured by making use of three different experimental sampling times, i.e., $\tau_{exp} = 28 \pm 2$, 45 ± 2, $70 \pm 2\ \mu s$. These data have been analyzed in exactly the same way as outlined in ref 8. This yields the energy dependence of the total rate constant $k_{tot} = \sum_i k^i$. In an approximative model, k_{tot} was equated to k^2, i.e., the rate constant of reaction 2, which represents the prevailing process below 13 eV and accounts for the lion's share of fragmentations below 11.7 eV, where some metastable parent ions can still be detected. If one anticipates that the two significantly less intense, competing processes 1 and 3 seem to involve very similar transition states as reaction 2, then the energy dependence of this approximate total rate constant gains significance, since it also provides a welcome link to earlier experimental[5] and theoretical[5,19] work where the presence of reaction 1 and 3 had been ignored completely. Relying on this "zeroth order" approximation, we can describe the decay of 1,3-butadiene cation very well by means of RRKM calculations. The experimental parent-ion breakdown data can be nicely reproduced with only little dependence on the details of the transition-state models used as long as the 1,3-butadiene cation $\tilde{X}\ ^2B_g$ structure is assigned to the reactant. A typical example revealing the agreement between computed and measured values is depicted in Figure 1. When linear and cyclic transition-state structures and σ values of 1 and 2 were employed, a family of 12 rate–energy functions was obtained. These functions yield 0 K threshold energies between 11.270 and 11.310 eV and F values around unity. The individual rate–energy functions show close agreement within the ionization energy range where experimental data for the parent ion can be obtained (cf. Figure 2). When these functions are extrapolated to significantly higher excitation energies, the spread increases, reaching about 1 order of magnitude at 13 eV.

Though only approximate, the rate–energy data presented in Figure 2 already reveal two noteworthy aspects. First, the rate rises from its threshold value of $\sim 5 \times 10^2\ s^{-1}$ to $\sim 5 \times 10^5\ s^{-1}$, i.e., about 3 orders of magnitude, within the first four-tenths of an electronvolt. This behavior is quite typical in view of the size of the species involved, the magnitude of the critical energy, and

(16) Maier, J. P. "Kinetics of Ion–Molecule Reactions"; Ausloos, P., Ed.; Plenum Press: New York, 1979.
(17) Shimanouchi, T. *Natl. Std. Ref. Data Ser. (U.S., Natl. Bur. Stand.)* **1972**, *39*.
(18) Mitchell, R. W.; Merritt, J. A. *Spectrochim. Acta, Part A* **1969**, *25A*, 1881.
(19) Chesnavich, W. J.; Bowers, M. T. *J. Am. Chem. Soc.* **1977**, *99*, 1705.

Table II. Parameters and Derived Quantities As Obtained from the RRKM Analysis of the Coincidence Data[a]

i[b]	ionic fragment	$E_0{}^i$,[c] eV	0 K threshold energy,[d] eV	$\Delta_f H^\ominus{}_0$(g), kJ mol^{-1}	F^i[f]	$\Delta S^\ddagger{}_{1000\,K}$,[g] cal deg^{-1}	$A_{1000\,K}$,[h] s^{-1}	$A_{classical}$,[i] s^{-1}
1	$C_4H_4^+$	2.530	11.590[j]	1252	1.102	−2.95	1.3×10^{13}	1×10^{13}
		2.580	11.640[j]	1247	1.170	−5.50	3.6×10^{12}	2×10^{12}
2	$C_3H_3^+$	2.215	11.275[k]	1066	1.006	−1.44	2.7×10^{13}	3.1×10^{13}
		2.210	11.270[k]	1065	1.026	−3.19	1.1×10^{13}	8.7×10^{12}
3	$C_4H_5^+$	2.355	11.415[k]	1009	1.008	−0.49	4.4×10^{13}	7.7×10^{13}
		2.365	11.425[k]	1010	1.047	−1.84	2.2×10^{13}	2.6×10^{13}

[a] The upper line for each fragment refers to a linear transition-state structure, the lower line to a cyclic one, see text. [b] Reaction number, see text. [c] 0 K critical energy of reaction, see text. [d] Calculated from $E_0{}^i$ and the adiabatic ionization energy of 1,3-butadiene, 9.060 eV. [e] This work. [f] Frequency change factor of reaction i, see text. [g] Equivalent activation entropy at 1000 K. [h] Equivalent preexponential factor at 1000 K. [i] Classical A factor. [j] ±0.2 eV. [k] ±0.1 eV.

the seemingly unreduced ($F \approx 1$, see also below) bonding in the transition state, relative to the precursor. Second, the values of the total rate constant in the vicinity of the thermodynamic (≈ 12.25 eV) and experimental (12.55 eV) threshold of reaction 4 are estimated to be $\sim 10^7$ s^{-1} and 5×10^7 s^{-1}, respectively. Presupposing that 1,3-butadiene cation $\tilde{X}\ ^2B_g$ represents also the reactant for process 4, the critical energy $E_0{}^4$ is larger than 3 eV, leading to a minimum rate on the order of ~ 1 s^{-1} at the thermochemical threshold. When the rate–energy function for $C_2H_4^+$ formation is computed by using transition-state parameters similar to those of the other three reactions, a value of $k^4 \approx 10^3$ s^{-1} is obtained at the experimental onset, corresponding to a 1000-fold increase of k^4 within 0.3 eV. However, if effective competition of all four processes on the ground-state manifold of 1,3-butadiene cation is assumed, a much more steeply rising rate–energy function is required in order to account for the measured branching ratios that amount to ~1% at the experimental threshold. Only an extremely loose transition-state model, which is rather unlikely to apply to reaction 4, would yield the demanded rate of $k^4 \approx 10^6$ s^{-1} at 12.55 eV, equivalent to an increase of 6 orders of magnitude for an excess energy of as little as 0.3 eV. Even the use of such an improbable transition-state model could not explain the experimental data, although it provides the required value of k^4 at the experimental onset, because k^4 would continue to rise exceedingly steeply at higher energies. As a consequence, formation of the other three product ions would be completely quenched within a few tenths of an electron volt above the measured onset energy of reaction 4, in obvious disagreement with the experimental breakdown diagram. Since the more detailed analysis relying on the fragment ion data (see below) essentially corroborates the results given in Figure 2, it must be concluded that reaction 4 is not in effective competition with the other three processes. Consequently, the energy dependence of k^4 could not be established in the course of this work.

E. Results Derived from the Fragment Ion Data. The coincidence data for $C_4H_4^+$, $C_4H_5^+$, and $C_3H_3^+$ formation can be properly explained by means of RRKM calculations of competitive unimolecular reactions taking place on the ground-state manifold of 1,3-butadiene cation. On the other hand, all efforts to include, in addition, reaction 4 as a further competitive dissociation channel failed for the reasons given above. Therefore, reaction 4 had to be excluded, and the experimental data were renormalized between 12.55 and 12.95 eV according to the number of molecular ions that dissociate into $C_4H_4^+$, $C_4H_5^+$, and $C_3H_3^+$ fragment ions. These data were then subject to rigorous RRKM calculations using expressions for k^i $(E^* - E_0{}^i)$ as given above and computation, convolution, and fitting procedures as stated. The calculations were carried out by employing linear and cyclic transition-state structures. Note, that the outcome of the respective calculations was the same when either the entire renormalized data set was used or the calculations were confined to energies not exceeding 12.25 eV, i.e., the thermochemical dissociation limit of reaction 4. The degree of accord between computed and measured breakdown data is virtually the same for the two transition-state models, but distinct values for the fit parameters are obtained (cf. Table II). The result of the calculations using a linear transition-state structure is compared with the experimental values in Figure 3. The rate–energy functions of the three processes

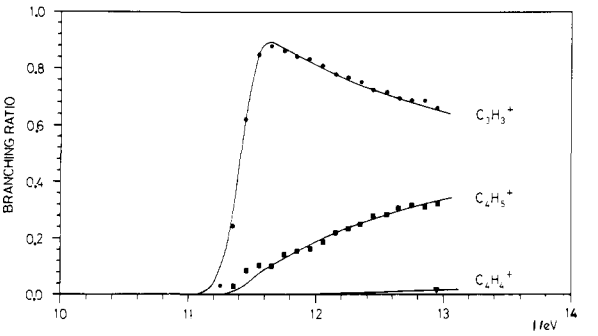

Figure 3. Experimental and calculated breakdown data for the three competing processes indicated, relying on a linear transition-state model.

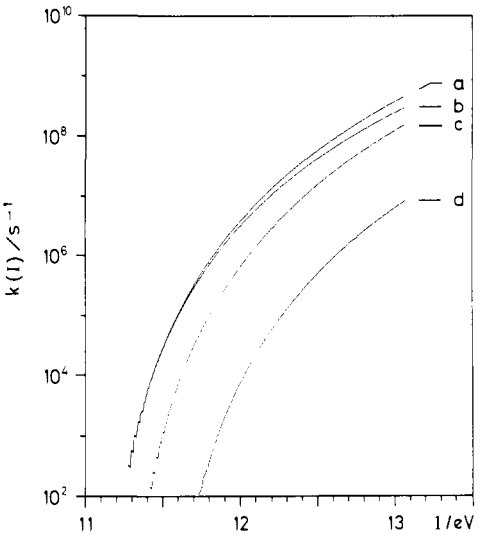

Figure 4. Total (a) and individual [(b) $C_3H_3^+$, (c) $C_4H_5^+$, (d) $C_4H_4^+$] best fit rate–energy functions corresponding to the breakdown curves given in Figure 3.

corresponding to these breakdown curves are presented in Figure 4.

Referring to the results of the present work collected in Table II, the critical energies increase in the series of fragmentation reactions 2, 3, and 1. Since the lowest thermochemical dissociation limit (cf. Table I) is unquestionably associated with $C_4H_4^+$ formation, this implies a substantial energy barrier on the order of 0.5 eV for the reverse process of reaction 1. Reverse activation energies of comparable magnitude have been reported for other ionic fragmentations that also involve the elimination of an H_2 molecule.[20] The detection of $C_4H_4^+$ fragments is strongly impeded by the other two competing reactions, which proceed much more rapidly (cf. Figure 4). This leads in particular to a substantial competitive shift[21] for the threshold energy of reaction 1 so that

(20) Bombach, R.; Dannacher, J.; Stadelmann, J.-P.; Vogt., J. *Chem. Phys. Lett.* **1980**, *76*, 429.

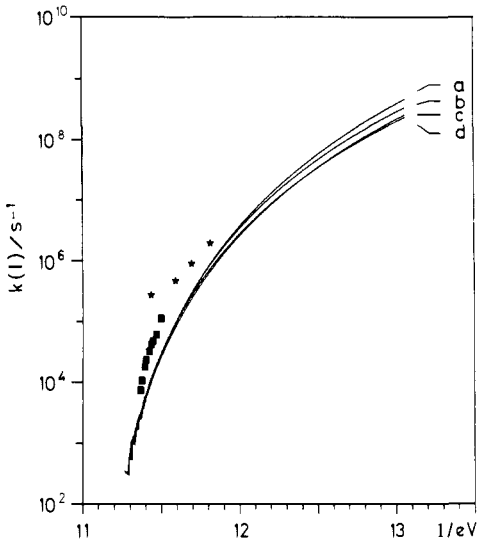

Figure 5. Best fit total rate–energy functions obtained from the complete analysis of the fragment ion data, using a linear (a) and a cyclic (c) transition-state model. Approximate rate–energy functions stemming from molecular ion data for linear (b) and cyclic (d) transition-state models. Rate–energy dependences reported in ref 5 (*) and 15 (■).

the experimentally observed onset (12.95 ± 0.1 eV) becomes practically meaningless. In such a case, only a detailed analysis of the breakdown diagram makes it possible at all to derive a reasonable value for the threshold energy. The present study yields a 0 K threshold energy of 11.6 ± 0.2 eV for reaction 1.

The 0 K threshold energies for the other two reactions could be determined more accurately, as competitive and kinetic shift effects are negligible. The two transition-state models used yield only slightly different critical energies for both reactions (cf. Table II). The coincidence data suggest that the kinetic energy release is insignificant at the threshold for both processes. Therefore, reliable values for the enthalpies of formation of $C_3H_3^+$ and $C_4H_5^+$ can be established, involving error limits of ±10 kJ mol^{-1}, assuming that none of the fragments is internally excited and their rotational energy is negligible.

The derived F values are remarkably large for $i = 1$ and slightly higher than unity for $i = 2$ or 3. This implies that the respective transition states are significantly ($i = 1$) and still slightly ($i = 2, 3$) tighter than the excited reactant. Accordingly, the formally inferred activation entropies at 1000 K are negative quantities. This is consistent with the known structure[22] of the three fragment ions at thresholds involving a cyclopropenium moiety which has to be formed in the course of the corresponding fragmentation processes. Since reaction 1 requires an H_2 molecule as the neutral fragment, its particularly tight transition state relative to the other two processes where an H or a CH_3 radical is eliminated is not surprising.

The outcome of the present study is compared with earlier data in Figure 5. Adding up the individual rate–energy functions of the three processes, our best estimate for the energy dependence of the total-decay rate constant is obtained. The rates predicted by the two different transition-state models differ by less than a factor of two at $I = 13$ eV and show even better agreement at lower energies. Since reaction 2 is the dominant fragmentation channel and the transition states for processes 2 and 3 are similarly "tight", the approximate (see above) rate–energy dependencies derived from the parent-ion data fall within the margins of error of the result of the exact treatment. Therefore, the serious discrepancy between measured and calculated rates reported earlier[5] cannot be due to the neglect of reaction 3 in the QET model used in that study but is rather a consequence of the improper method of coincidence data analysis. Since the origin of this artefact appears to be clear now,[10] it is redundant to comment further on these earlier experimental values that are much too high, in particular in the threshold region. The present study also amends our own earlier results[15] where the initial thermal energy content of the photoionized molecules was ignored, effecting too high values for the rate constant.

Conclusions

The decay processes of excited radical cations can be described quantitatively when photoelectron–photoion coincidence spectroscopy and RRKM theory of unimolecular reactions are combined on mutual terms. Assuming a series of competitive unimolecular reactions, the measured, properly normalized breakdown diagram is completely determined by the rates of the fragmentations involved and their dependence on the available excess energy as well as the effective sampling function of the coincidence experiment. This latter quantity depends on the thermal energy content of the photoionized molecules and the electron transmission function of the coincidence spectrometer. In order to derive the rate–energy dependencies of the competing dissociations from the observed breakdown diagram, we must take into account this sampling function and a mathematical model for the energy dependence of the rate constants is required. If one relies on RRKM theory and its underlying assumptions, such a model can be defined in a very simple and straightforward way. After particular sets of frequencies have been assigned to the reactant and to the transition state, a standard fitting procedure connecting the calculated data with the experimental results can be used to determine those values of the parameters that yield maximum agreement between theory and experiment. Varying merely the critical energy of reaction and a multiplier for the ensemble of transition-state frequencies for each process achieves good accord between measurement and computation. On the basis of this simple RRKM model, the finer details of the decay processes can then be probed. This method can be used to establish threshold energies even when kinetic and/or competitive shift effects are involved. It also provides information on the presence or absence of effective competition among the various fragmentation reactions. Moreover, it allows some qualitative statements about the degree of bonding in the transition state relative to the precursor. It is further possible to transfer the derived rate–energy functions to comparable neutral systems where unimolecular fragmentations can rarely be studied under collision-free conditions. This important link might then be used to test the different activation and deactivation models used in classical kinetics.

Acknowledgment. This work is part C25 of project 2.017-081 of the Schweizerischer Nationalfonds zur Förderung der wissenschaftlichen Forschung (part C24: cf. ref 27). Support by Ciba-Geigy SA, F. Hoffmann-La Roche, and Cie. SA and Sandoz SA (Basel) is gratefully acknowledged. J. D. thanks the Max Geldner Stiftung for financial support.

Registry No. 1,3-Butadiene, 106-99-0; 1,3-butadiene radical cation, 34488-62-5.

(21) McLafferty, F. W.; Wachs, T.; Lifshitz, C.; Innorta, G.; Irving, P. *J. Am. Chem. Soc.* **1970**, *92*, 6867.
(22) Rosenstock, H. M.; Dannacher, J.; Liebman, J. F. *Radiat. Phys. Chem.* **1982**, *20*, 7.
(23) Rosenstock, H. M.; Draxl, K.; Steiner, B. W.; Herron, J. T. *J. Phys. Chem. Ref. Data Suppl. 1* **1977**, *6*.
(24) Stull, D. R.; Prophet, H. JANAF Thermochemical Tables, 2nd ed., NSRDS-NBS 37, U.S. Department of Commerce, June 1971.
(25) Wiberg, K. B.; Fenoglio, R. A. *J. Am. Chem. Soc.* **1963**, *90*, 3395.
(26) Rosenstock, H. M.; Stockbauer, R.; Parr, A. C. *Int. J. Mass Spectrom. Ion Phys.* **1981**, *38*, 323.
(27) Bombach, R.; Stadelmann, J.-P.; Vogt, J. *Chem. Phys.* **1982**, *72*, 259.